Orientation of Cross-Linked Poly(vinylidene fluoride) Crystallized from Oriented Amorphous Melts

K. S. Spector and R. S. Stein*

Polymer Research Institute, University of Massachusetts, Amherst, Massachusetts 01003

Received June 11, 1990; Revised Manuscript Received November 1, 1990

ABSTRACT: Radiation cross-linked samples of poly(vinylidene fluoride) (PVF_2), obtained from the Raychem Corp., were heated to above their crystalline melting point, stretched, and isothermally recrystallized at 100 °C. The crystalline and amorphous orientation functions were studied as a function of cross-link density and extension ratio by X-ray diffraction and birefringence. The crystalline phase orients with its *c* axis parallel to the deformation direction, and the amorphous phase orients perpendicular to this direction. The degree of orientation of both the crystalline and amorphous phases increases with cross-link density and with extension ratio. Intrinsic birefringence values for both the crystalline and amorphous phases of PVF_2 are offered. The intrinsic birefringence of the amorphous phase, calculated from bond polarizabilities and birefringence measurements using rubber elasticity theory, is 0.098 ± 0.017. The intrinsic birefringence of the α crystalline phase as calculated from bond polarizabilities using the differentiated Lorentz–Lorenz equation is 0.145 ± 0.002. Each sample is characterized in terms of its polymorphic form by wide-angle X-ray diffraction, its molecular weight using Flory–Rehner theory, and the degree of crystallinity from density measurements. In addition, a value of $\chi = 0.15$ is offered for the polymer–solvent interaction parameter in *N,N*-dimethylacetamide. Finally, attempts at drawing a correlation between the amorphous orientation functions of molten PVF_2 samples and the orientation functions of these same samples after crystallization indicate that the crystalline orientation functions indeed depend upon the amorphous orientation functions of the deformed molten network rather than upon the cross-link density or extension ratio of the samples taken separately.

Introduction

As with many polymers, several important physical properties of poly(vinylidene fluoride) (PVF_2) arise and are affected during processing. Specifically, stretching and poling can convert a low-technology allotment of PVF_2 into a valuable high-technology piezoelectric and pyroelectric material. This metamorphosis is a direct result of the molecular and dipolar orientation brought about by the stretching and poling process. The crystal structure of PVF_2 is highly influenced by its thermal, mechanical, and electrical history. Under appropriate conditions four different polymorphs can be found referred to as α (phase 2), β (phase 1), γ (phase 3), and δ (phase 4).[1] The α crystalline phase is the most common and is created by melt crystallization at moderate to high undercoolings. The β phase is the most commercially important form of PVF_2 since it can be made to possess the valuable piezoelectric and pyroelectric properties through the stretching and poling process. The β phase is usually formed by recrystallizing at low undercoolings or by deforming the α crystalline phase.

In this laboratory, the two components of processing, mechanical and electrical, have been studied separately in order to obtain a clearer picture of how each affects crystallization and orientation. The crystallization of PVF_2 in the presence of low electric fields has been examined by Marand,[2] who found the γ phase to preferentially form in the presence of an electric field with an increase in the crystal nucleation rate and content with increasing field strength. The present work is devoted to the mechanical component of polymer processing. Specifically, the crystalline phase and the orientation of both the amorphous and crystalline regions of the polymer are examined after deformation in the melt.

Experiments have shown that lightly cross-linked polymers that are melt crystallized and subsequently deformed in the solid state possess different morphologies and properties from samples that are deformed in the molten state and then recrystallized.[3,4] Part I of this study shows the unique orientation characteristics of PVF_2 when oriented in the molten state; i.e., the amorphous phase orients perpendicular to the deformation direction, while the *c* axis of the crystalline regions orient along the deformation direction.

Part II of this work suggests a relationship between the crystalline orientation function of the crystals, and the statistical segment of the molten precursor. Plots of crystalline orientation versus extension ratio are given which indicate that the crystal orientation depends on the extension ratio of the melt before crystallization. In addition, the plots for the more highly cross-linked samples show more orientation than the lower cross-linked samples. Clearly, the crystalline orientation depends on both the extension ratio and the cross-link density of the molten deformed precursor from which the semicrystalline samples are prepared. Several experiments by Kawai[5] and others[6] have also indicated that the orientation of a semicrystalline polymer depends on the orientation of the molten precursor rather than on the extension ratio or cross-link density taken separately. In particular, studies by Forgacs and Stein in this laboratory on linear low-density polyethylene support this conclusion. However, one may ask about the exact nature of this dependence. Does the crystalline orientation increase directly with extension ratio, with some power of the extension ratio or in a more complicated fashion? What are the limits of this dependence? Is it the same at low extensions as at high extensions? These same questions may be asked of the cross-link density, and all are important if one wants to predict the amount of crystalline orientation that a particular set of processing conditions will produce. This work attempts to answer these questions by showing that the crystalline orientation of PVF_2 depends upon the statistical segment orientation prior to crystallization as Kawai and Forgacs has suggested for polyethylene; i.e., the crystalline orientation is a function of the quantity $f_{\text{stat seg}} = [1/5n_s][\lambda^2 - 1/\lambda]$, where λ is the extension ratio and n_s is the number of statistical segments between cross-

0024-9297/91/2224-2083$02.50/0 © 1991 American Chemical Society

links.[7] Lastly, efforts will be made to determine if the crystalline orientation depends on the amorphous orientation of the whole melt (the soluble fraction plus gel) or just the cross-linked network.

Experimental Section

Sample Preparation. Radiation cross-linked films of Solvay Soles 1008 PVF_2 obtained from the Raychem Corp. are heated to above their crystalline melting point (200 °C), stretched, and isothermally recrystallized at 100 °C under constant strain. The suspension-polymerized samples were cross-linked by an electron beam in air at room temperature and contain <5% head-to-head and tail-to-tail units. Samples of two different cross-link densities are examined in all experiments and are cross-linked with radiation doses of 3 Mrad (MR) and 6 Mrad, respectively. The cross-link density and gel fraction of the samples are 5×10^{-5} mol/cm^3 (70% gel) and 1×10^{-4} mol/cm^3 (80% gel) for the 3MR and 6MR samples, respectively, as determined from swelling experiments.

According to Flory–Rehner theory,[8] the average cross-link density (density/molecular weight) of an elastic network at swelling equilibrium can be calculated from the equation

$$[\ln (1 - \phi_2) + \phi_2 + \chi_1\phi_2 + (d_2V_1/M_c)(\phi_2^{1/3} - \phi_2/2)] = 0 \quad (1)$$

where ϕ_2 and d_2 are the volume fraction and density of the polymer, respectively, V_1 is the partial molar volume of the solvent, and χ_1 is the Huggins constant. The volume fraction of the extracted samples is measured in the solvent *N,N*-dimethylacetamide ($V_1 = 93.02$ cm^3/mol) at 100 °C. Unfortunately, the polymer–solvent interaction parameter (Huggins constant) was not previously known for PVF_2 so it was calculated from eq 1 by measuring the volume fraction of PVF_2 samples having known molecular weights. A value of $\chi_1 = 0.15$ is calculated for the Huggins constant at 100 °C, which corresponds to a good solvent according to the theory of polymer solutions. This is supported by the experiences of many investigators who have found dimethylacetamide to be a good solvent for PVF_2.

Part I: Crystal Structure and Orientation

X-ray Diffraction. Crystalline Structure. Debye–Scherrer powder photographs taken with a Statton flat-film camera proved useful in determining the unit cell of the samples as well as in providing a qualitative look at orientation. Utilizing the Bragg equation, $n\lambda = 2d \sin\theta$, the d spacings are measured and by comparing with the literature a determination of the crystalline unit cell present is made.[9,10] The broad amorphous halo may also be seen.

Crystalline Orientation. It is common to describe the degree of orientation by the Hermans–Stein orientation functions,[11,12] which have the form

$$f = [3\langle\cos^2\phi_{hkl}\rangle - 1]/2 \quad (2)$$

where ϕ is the angle between the normal of a crystalline plane and the direction of interest, which is usually the deformation direction. The quantity $\langle\cos^2\phi_{hkl}\rangle$ is an average over all the crystallites in a sample. The orientation function ranges from 0 for random orientation to 1 for perfect orientation or −1/2 for perpendicular orientation.

Measuring $\langle\cos^2\phi_{hkl}\rangle$ by X-ray Diffraction. The value of $\langle\cos^2\phi_{hkl}\rangle$ is given by the relation

$$\langle\cos^2\phi_{hkl}\rangle = \frac{\int_0^{\pi} I(\phi)\sin\phi\cos^2\phi\,d\phi}{\int_0^{\pi} I(\phi)\sin\phi\,d\phi} \quad (3)$$

where $I(\phi)$ is the intensity diffracted by plane normals at a given azimuthal angle. Wilchinsky's method,[13] often employed to obtain a value for the c-axis orientation when it cannot be measured directly, is used to determine the mean square cosine due to the low intensities of the crystal planes required in the more direct approach. Due to the orthorhombic crystal structure of the α phase of PVF_2, it is necessary to measure only two crystal planes, the (020) and the (110).

In practice, an automated Siemens D-500 X-ray diffractometer is used for these measurements. The symmetrical transmission technique is employed using Cu Kα radiation. The essence of the method is to take radial $\theta/2\theta$ scans of each sample at several equally space azimuthal angles from 0 to 90°. The data are corrected for polarization, background intensity, and absorption by the sample. The amorphous intensity is then subtracted from the corrected crystalline intensities. Finally, one plots the intensity versus ϕ and the data are used in eq 3 to determine $\langle\cos^2\phi_{hkl}\rangle$.

Birefringence. Amorphous Orientation. Birefringence measures the total orientation of all phases of the system. The contribution of each phase to the total is determined by the relative amount of that phase and the intrinsic birefringence of the phase. For a uniaxially oriented system the birefringence is given by[14]

$$\Delta_n = \phi_{cr}\Delta^\circ_{cr}f_{cr} + (1 - \phi_{cr})\Delta^\circ_{am}f_{am} + \Delta_{form} \quad (4)$$

where Δ°_c and Δ°_{am} are the intrinsic birefringence values of the crystalline and amorphous phases, respectively, and ϕ_{cr} is the volume fraction crystallinity. The form birefringence Δ_{form} arises from the distortion of the electric field at phase boundaries and will be neglected. The amorphous orientation function f_{am} can be determined from eq 4 if the following conditions are met: (1) the form birefringence is neglected, (2) the crystal orientation function f_{cr} is known from an independent method such as X-ray diffraction, (3) the degree of crystallinity ϕ_{cr} is known from density measurements, and (4) the intrinsic birefringences are known. Unfortunately, the intrinsic birefringences of PVF_2 were not previously known, so the method outlined below is followed to determine them.

Intrinsic Birefringence of the Crystalline Phase. The intrinsic birefringence of the α crystalline phase of PVF_2 can be calculated by substituting the optical anisotropy of the unit cell, $(b_1 - b_2)$, into the differentiated Lorentz–Lorenz equation[15]

$$\Delta^\circ_c = [2\pi/9V][(n_0^2 + 2)^2/n_0](b_1 - b_2) \quad (5)$$

The Lorentz–Lorenz equation assumes the molecule resides in a spherical cavity of uniform internal field. The optical anisotropy of the unit cell is calculated from bond polarizabilities with the assumption that they are additive.

Intrinsic Birefringence of the Amorphous Phase. For a lightly cross-linked polymer the intrinsic birefringence of the amorphous phase can be found by relating birefringence and rubber elasticity theory.[16] PVF_2 in the melt will be totally amorphous, resulting in the simplification of eq 4 to

$$\Delta_n = \Delta^\circ_{am}f_{am} \quad (6)$$

Furthermore, the orientation of a statistical segment in a pure amorphous network is given by the Kuhn–Grun theory to be

$$f = [1/5n_s][\lambda^2 - 1/\lambda] \quad (7)$$

where λ is the extension ratio of the network and n_s is the number of statistical segments between cross-links. It is apparent that by combining eq 6 and 7 the intrinsic birefringence can be indirectly measured through Δ_n, λ, and n_s.

In eq 7 n_s is the number of statistical segments per chain, which can be expressed as $n_s = M_c/ZM_m$, where Z is the number of monomer units per segment. Z is calculated by means of the stress optical coefficient in the following way. First, assuming bond polarizabilities are additive, Z should equal the ratio of the statistical segment and monomer anisotropies as follows:

$$Z = (\alpha_1 - \alpha_2)/(b_l - b_t) \tag{8}$$

The monomber anisotropy, $(b_l - b_t)$, is found from the geometry of the monomer unit and from bond polarizabilities available in the literature through the following transformation equations:[17]

$$\alpha_{xx} = \alpha_1 \cos^2\theta + \alpha_2 \sin^2\theta$$

$$\alpha_{yy} = (\alpha_1 - \alpha_2) \sin^2\theta \cos^2\phi + \alpha_2$$

$$\alpha_{zz} = (\alpha_1 - \alpha_2) \sin^2\theta \sin^2\phi + \alpha_2$$

$$\alpha_{xy} = \alpha_{yx} = (\alpha_1 - \alpha_2) \sin\theta \cos\theta \cos\phi$$

$$\alpha_{zy} = \alpha_{yz} = (\alpha_1 - \alpha_2) \sin^2\theta \sin\phi \cos\phi$$

$$\alpha_{zx} = \alpha_{xz} = (\alpha_1 - \alpha_2) \sin\theta \cos\phi \sin\phi \tag{9}$$

The quantity $(\alpha_1 - \alpha_2)$ may be found from the stress-optical coefficient

$$C = \Delta/\sigma = [2\pi/45kT][(n_0^2 + 2)/n_0](\alpha_1 - \alpha_2) \tag{10}$$

Therefore, by measuring birefringence as a function of stress in the melt C may be determined. The calculation of Z relies on the assumption that bond polarizabilities are additive, which is not strictly true. A difficult but possibly more realistic calculation of Z can be found from statistical mechanics as proposed by Flory.[18]

Molecular Weight between Cross-Links. According to the theory of rubber elasticity[7] $\sigma = RT/M_c(\lambda^2 - 1/\lambda)$; therefore, the molecular weight of a cross-linked network can be found from plots of stress versus the quantity $(\lambda^2 - 1/\lambda)$ for samples in the melt. The molecular weight between cross-links of the samples used in these experiments is about 15 000 and 30 000 for the 6MR and 3MR samples, respectively.

Part II: Dependence of the Crystalline Orientation Function on the Amorphous Orientation Function of the Molten Precursor

Radiation Dose and Extension Ratio Dependence of the Statistical Segment Orientation. According to rubber elasticity theory, the amorphous orientation of statistical segments in a Gaussian cross-linked network is given by the well-known equation of Kuhn,[7] $f_{stat\ seg} = [1/5n_s][\lambda^2 - 1/\lambda]$, where n_s is the number of statistical segments between cross-links and λ is the extension ratio. In the above equation n_s can be broken down to show that it contains the cross-link density dependence. The quantity n_s equals the molecular weight of the chain between cross-links divided by the monomer molecular weight and Z, the number of monomer units per statistical segment; i.e., $n_s = M_c/M_0Z$. Also, $M_c/M_0 = 1/Q_0r$, where Q_0 is the radiation cross-linking efficiency and r is the radiation dose. Therefore, substituting $1/Q_0rZ$ for n_s in the equation for $f_{stat\ seg}$ gives

$$f = \frac{M_0Z}{5M_c}[\lambda^2 - 1/\lambda] = \frac{Q_0rZ}{5}[\lambda^2 - 1/\lambda] \tag{11}$$

In eq 11 Q_0 and Z are constants and f depends on the radiation dose as well as the extension ratio. Since the statistical segment orientation function and the crystalline orientation function both depend on the radiation dose and the degree of extension, one may logically conclude that plots of f_c versus $f_{stat\ seg}$ should be superimposible for samples differing in cross-link density or extension ratio.

Effect of the Soluble Fraction on $f_{stat\ seg}$. The expression for $f_{stat\ seg}$ in eq 11 refers to the pure cross-linked network, i.e., the gel fraction of a lightly cross-linked sample. However, if the soluble fraction has not been extracted from the samples, then both the extension ratio and the molecular weight between cross-links will be replaced by the effective extension ratio λ' and the effective molecular weight M_c' of the sol plus gel. Clearly, the molecular weight between cross-links will be larger in the sol than in the gel. In addition, experiments have been done which indicate that the sol fraction may orient independently of the gel fraction, therefore implying that the extension ratio may be much larger in the gel than in the sol fraction.[19]

One may calculate the amorphous orientation function of the gel fraction using values of λ' and M_c' measured on the sol plus gel provided that the right-hand side of eq 11 is multiplied by the correction factor $(1 - S^2)$ suggested by Charlesby,[20] which accounts for the amount of sol in the network as well as the difference in the molecular weight between cross-links in the soluble fraction. The gel fraction is considered to consist of chains that are cross-linked by covalent bonds. The soluble fraction is considered to be made up of chains having no permanent cross-links, although entanglements may exist that act in a similar fashion.

This investigation attempts to show that the crystalline orientation of PVF_2 is determined by the amorphous orientation of the molten sample prior to crystallization rather than by the extension ratio or cross-link density taken separately. The crystalline orientation functions wil be plotted against both the amorphous orientation functions of the gel and the amorphous orientation functions of the whole molten precursor to determine which gives the best correlation. The superimposition of curves for samples differing in cross-link density would be indicative of a good agreement with theory.

The amorphous orientation functions for the whole system (sol plus gel) are calculated by means of eq 11 and the amorphous orientation functions for the gel fraction are calculated with the equation of Charlesby. The molecular weight between cross-links, M_c, and the soluble fraction of the lightly cross-linked network, S, have both been determined from swelling experiments. The values $M_0 = 64.0346$ g/mol and $Z = 1.2$ are also used. The amorphous orientation functions are plotted against the corresponding crystalline orientation functions and the 3MR plots are superimposed over those of the 6MR samples to evaluate the agreement with theory.

Results and Conclusions

Crystalline Phase. The observed data obtained from the Debye–Scherrer photographs on unoriented samples are given in Table I. The d spacings and intensities of the first nine rings correspond very closely to the literature values for the α-phase unit cell of PVF_2, which is orthorhombic with the dimensions $a = 4.96$, $b = 9.64$, and

Table I
X-ray Unit Cell Data[a]

ring no.	obsd	lit.	(*hkl*) plane	$I^{1/2}$
1	5.03	5.03	(100)	27.2
2	4.83	4.81	(020)	41.2
3	4.44	4.45	(110)	70.3
4	3.34	3.34	(021)	49.9
5	2.78	2.78	(121)	23.1
6	2.71	2.70	(130)	22.5
7	2.50	2.50	(200)	35.8
8	2.42	2.43	(210)	39.3
9	2.42	2.41	(040)	13.8

[a] Unit cell parameters: $a = 4.96$ Å, $b = 9.64$ Å, $c = 4.62$ Å, orthorhombic.

Table II
Hermans-Stein Orientation Functions

3MR Samples

	L/L_0		
	1.6	2.1	2.5
f_a	−0.06	−0.10	−0.02
f_b	−0.21	−0.25	−0.16
f_c	0.26	0.35	0.17

6MR Samples

	L/L_0		
	1.7	2.3	2.7
f_a	−0.26	−0.30	−0.33
f_b	−0.16	−0.22	−0.26
f_c	0.42	0.53	0.59

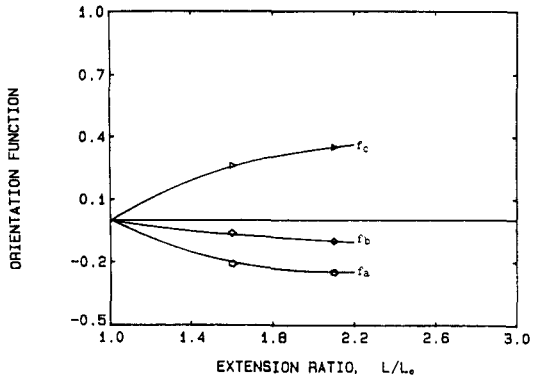

Figure 1. Relationship between the crystalline orientation functions and the extension ratio of the 3MR samples.

$c = 4.62$.[21] The unit cell belongs to the space group $P2_1/c\text{-}C_{2h}^5$ and contains chains of two monomer units in length, each having a TGTG′ conformation. Finding the α phase as the sole crystalline structure is reasonable since it is the phase usually obtained when crystallizing from the melt at high undercoolings, even in deformed samples. Above 150 °C one normally finds a mixture of the α and β phases. The reason for this is thought to be because the β phase is thermodynamically favored whereas the α phase is kinetically favored.[1,22] The data for the deformed samples also indicate α-phase crystallization.

Quantitative Evaluation of Crystal Orientation. The orientation functions were calculated by Wilchinsky's method using the (020) and (110) planes. The orientation functions are given in Table II for both the 3MR and 6MR samples. The results based on Wilchinsky's method are shown in graphical form in Figures 1 and 2 for the 3MR and 6MR samples. The following are general observations and conclusions based on these results.

(1) For both the 3MR and the 6MR samples the crystalline c axis orients parallel to the stretching direction,

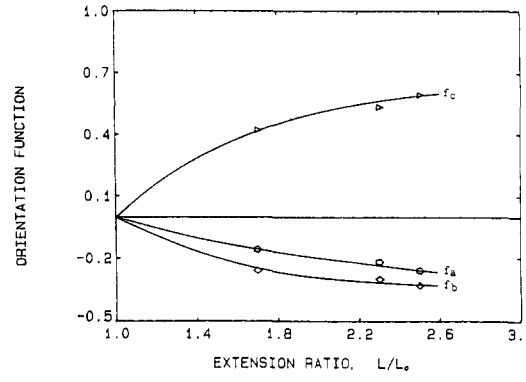

Figure 2. Relationship between the crystalline orientation functions and the extension ratio of the 6MR samples.

and the a and b axes orient perpendicular to the stretching direction, although not to equal extents.

(2) The orientation increases with the degree of extension of the molten samples.

(3) The increase in orientation is not linear but rather levels off before high degrees of orientation are reached.

(4) The 6MR samples orient approximately twice as efficiently as the 3MR samples.

Factors Affecting Total Quantity of Orientation. On the basis of the results of other polymers as well as the theory of rubber elasticity, one would probably expect the orientation to increase with extension ratio and with cross-link density.[13,14,16,23] The amount of orientation is relatively low even at high extensions as compared with samples that are stretched in the solid state. This is due to a fundamental difference in the orientation mechanism. In the solid state the van der Waals bonds that hold the crystals together prevent chain slipping during extension so the orientation is more effective. In addition, the high internal energy of the melt favors chain relaxation back into the random unoriented state. It is the chain slipping that undoubtedly causes the leveling off of the orientation at high extensions.

Below the gel point cross-links hold the network together and prevent relaxation, so it is reasonable to find that the orientation increases with cross-link density. In fact, rubber elasticity theory predicts that the amorphous orientation of the 6MR molten network should be twice as large as the amorphous orientation of the 3MR molten network.[7] The results of these experiments indicate that the amorphous orientation carries over to the crystal orientation since the crystalline orientation of the 6MR samples is twice as large as the crystalline orientation of the 3MR samples.

Relative Amounts of *a*-, *b*-, and *c*-Axis Orientation. One would expect the chain axis to orient with the stretching direction as occurs in these experiments; however, it should not be taken for granted that this will always occur since the crystal orientation process is affected by the organization of the crystals in superstructures such as spherulites. For example, polyethylene will have a-axis orientation at low extensions, although this will convert to c-axis orientation at higher extensions.[24] Also, considering the orthorhombic symmetry of the unit cell, it is necessary for the a and b axes to orient perpendicular to the stretching direction if the c axis orients along the stretching direction.

An interesting observation is that the a axis orients less than the b axis in the 3MR samples, whereas in the 6MR samples the a axis orients more than the b axis. Indeed, the b-axis orientation seems to remain about the same in

both sets of samples. These results can be explained if one considers the details of crystallization from a deformed melt.

Crystallization of strained melts often results in row-nucleated structures where linear nuclei are formed parallel to the strain direction.[25-27] The epitaxial growth on the surface of these row nuclei produce folded-chain lamellae which are oriented with their c axes parallel to the strain direction and their a and b axes oriented perpendicular to the deformation direction with spherical symmetry. Now consider what the effect would be on orientation if the growing lamellae exhibited a helical twist. Crystallization under low stress would produce primary nuclei made up of more or less extended polymer chains having their c axes oriented in the direction of strain and having a and b axes oriented in the plane perpendicular to the deformation direction. If the lamellae formed from the epitaxial growth on these nuclei twist, then the c and a axes will be randomly oriented around the axis of maximum growth rate (the b axis in the case of PVF_2), which itself will be oriented perpendicular to the strain direction. The net result one would expect from this situation is a small c-axis orientation along the strain direction from the oriented primary nuclei and a small b-axis orientation perpendicular to the strain resulting from the epitaxial lamellar growth. The a axis should have relatively little orientation. These are indeed the results that are obtained for the 3MR samples. Furthermore, the assumption that the lamellae possess a twist period is supported by Lovinger's finding that the α phase crystallizes from the melt in the form of banded spherulites having a small twist period of about 1 μm per 180°.[28]

The higher stresses that exist in the 6MR samples do not allow for the helical twisting that occurs in the 3MR samples. For this reason the 6MR samples orient with both their a and b axes perpendicular to the deformation direction and the c axis parallel to the deformation direction. Both sets of samples, however, would be expected to possess cylindrical symmetry due to being only uniaxially oriented. This means that the a and b axes are randomly oriented in the plane perpendicular to the deformation direction.

Intrinsic Birefringence of PVF_2. The intrinsic birefringence of the crystalline phase is 0.145 ± 0.002 as determined from the differentiated Lorentz–Lorenz equation using additivity of bond polarizabilities. This method is approximate and depends on the values chosen for the bond polarizabilities. By comparison the intrinsic birefringence of isotactic polypropylene crystals is 0.029, much lower than for PVF_2. The difference is due to the relatively greater anisotropy of the vinylidene fluoride monomer and perhaps to a difference in the anisotropy of the unit cells. The effect of anisotropy of the internal field is neglected in this calculation.

The intrinsic birefringence of the amorphous phase of PVF_2 can be calculated from eq 6–8, using 64 0346 g/mol for M_0, 39 000 g/mol for M_c, and the values Z = 1.22 and Z = 1.20 for the 3MR and 6MR samples, respectively.

An average value of 0.092 ± 0.017 is found for the amorphous intrinsic birefringence of the 3MR samples, with values varying from 0.11 to 0.075. An average value of 0.098 is found for the 6MR samples, with values ranging from 0.11 to 0.088. In both sets of samples the intrinsic birefringence tends to decrease with increasing extension. This is most probably due to an increase in the packing density of the chains with increasing extension, which will affect the internal field. A value of 0.1 is found for the intrinsic birefringence of the amorphous phase using the differentiated Lorentz–Lorenz equation as was done for the intrinsic birefringence of the crystalline phase. Although this method is approximate, the close agreement with the previously stated values lends greater confidence to these results. For comparison the intrinsic birefringence of the amorphous phase of isotactic polypropylene is 0.060. One would probably expect PVF_2 to have a higher intrinsic birefringence than polypropylene because the fluorines attached to the hydrocarbon chain make it more anisotropic than polypropylene.

Table III
Degree of Crystallinity from Density Measurements

sample	wt, g	ρ, g/cm^3	deg of cryst, %
6MR, L = 1.7	65.5903	1.7614	49
6MR, L = 2.3	65.5252	1.7585	48
6MR, L = 2.7	65.6916	1.7659	51
3MR, L = 1.6	65.6573	1.7644	51
3MR, L = 2.1	65.6683	1.7649	51
3MR, L = 2.5	66.0425	1.7814	58

The intrinsic birefringence can be thought of as the birefringence of a perfectly oriented phase (i.e., with f = 1), be it either crystalline or amorphous. The difference between the two is due to the difference in the internal field that the two phases experience, for a bond will experience not only the electromagnetic field of the incident light but also the net polarization of its surroundings. There are three factors that influence this internal field and they are (1) the packing density of the chains, (2) the environment of the chains (surrounded by an amorphous phase, a crystalline phase, or both), and (3) the anisotropy of the surroundings. Stein and Vuks have derived theories for the internal field of the polyethylene crystal.[29,30]

Amorphous Orientation of Deformed Semicrystalline PVF_2 Samples. The amorphous orientation of PVF_2 samples that were deformed in the melt and subsequently recrystallized has been calculated with eq 14 using the values 0.145 and 0.092 for the intrinsic birefringences of the α crystalline and amorphous phases, respectively. The volume fraction degree of crystallinity for these samples, given in Table III, have been calculated from density measurements. The pure amorphous and crystalline densities at 20 °C are 1.68 and 1.92 g/cm^3, respectively.[1,9]

The amorphous phase orients perpendicular to the deformation direction and increases with both the cross-link density and the extension ratio. This result might seem surprising at first since one would expect the stretching of the melt to align the molecular chains along the deformation direction. However, the chains that do orient along the deformation direction fall into the more stable crystalline phase upon cooling the melt, thereby leaving the remaining chains oriented in a perpendicular direction. In addition, the growing crystals possibly compress the interlamellar noncrystallizable regions into a perpendicular orientation. Lastly, the chain folds must also be oriented perpendicular to the oriented crystals. Therefore these results indicate that the amorphous orientation is associated with the crystalline orientation. If this were the case, one would expect the amorphous orientation to become more negative as the crystalline orientation becomes more positive, and this is indeed observed. Since the higher cross-linked samples have more crystalline orientation, there is also a corresponding increase in the amorphous orientation.

Theoretical Relationship between the Crystalline and Amorphous Orientation Functions. While it is known that the crystalline orientation is a function of both

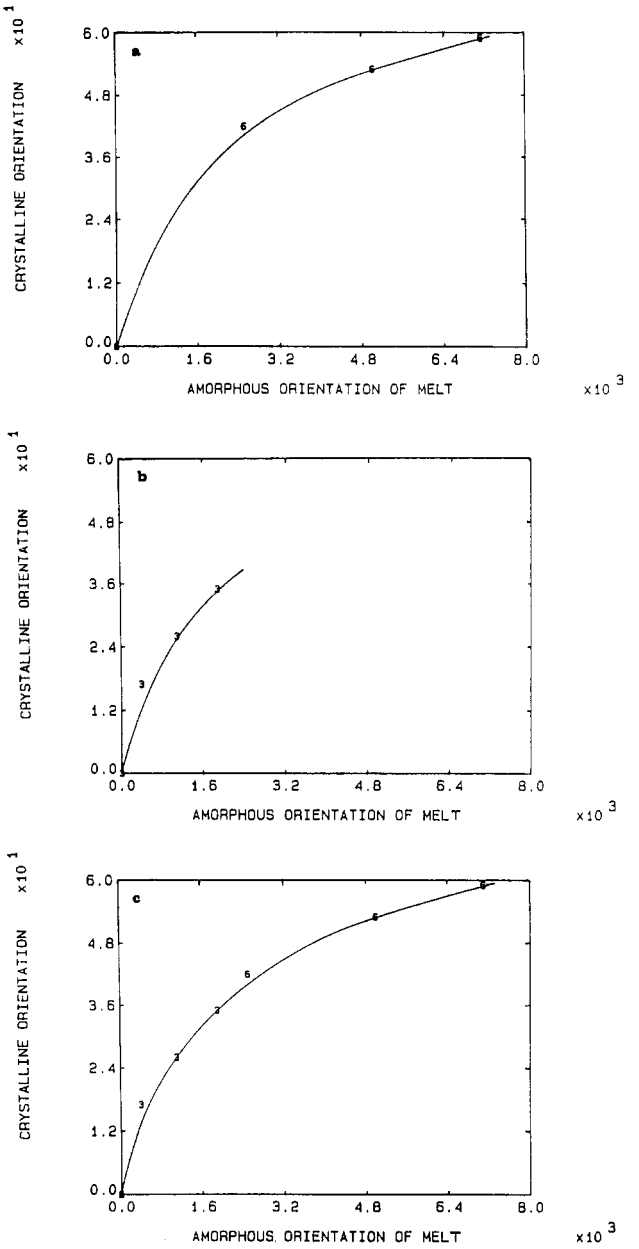

Figure 3. Relationship between the crystalline orientation functions and the amorphous orientation functions of the whole molten precursor (sol + gel): (a) the higher cross-linked samples; (b) the lower cross-linked samples; (c) the higher and lower cross-linked samples superimposed.

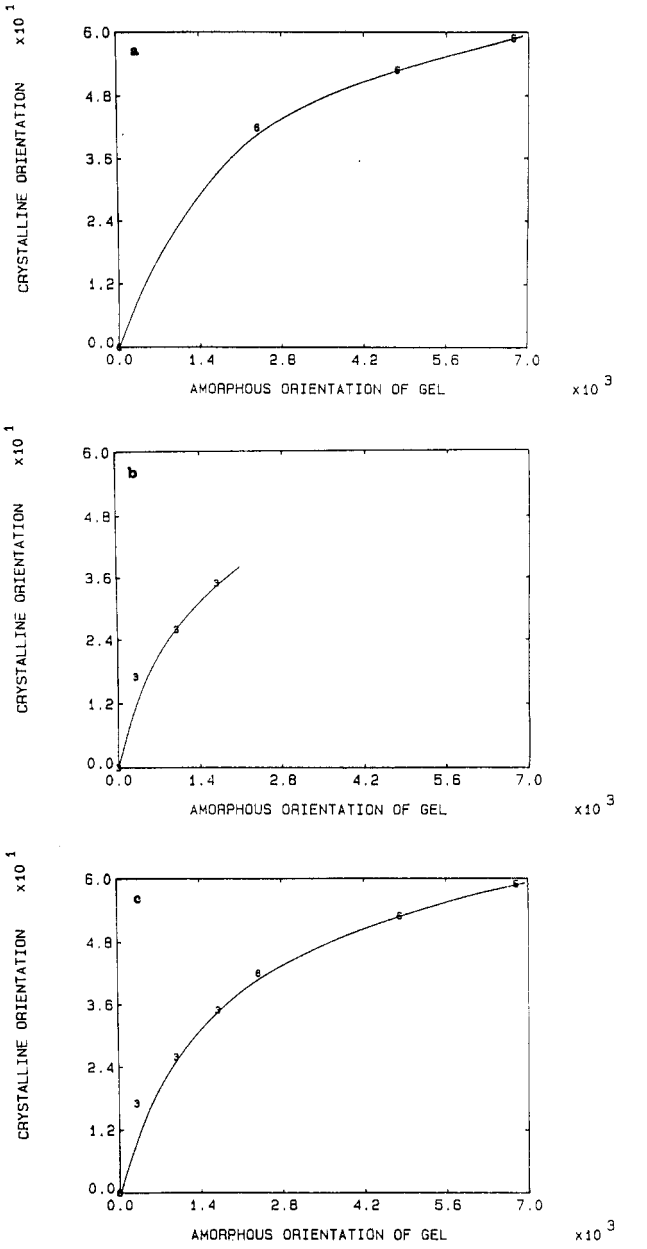

Figure 4. Relationship between the crystalline orientation functions and the amorphous orientation functions of the molten gel: (a) the higher cross-linked samples; (b) the lower cross-linked samples; (c) the higher and lower cross-linked samples superimposed.

the extension ratio and the cross-link density, confirming that the crystalline orientation depends upon the amorphous orientation prior to crystallization gives the exact nature of that dependence; i.e., the crystalline orientation depends on the quantities $(\lambda^2 - 1/\lambda)$ and $1/M_c$.

According to eq 11 the same degree of amorphous orientation can be produced by samples differing in extension ratio, providing the cross-link densities of the samples also differ by an appropriate amount. Therefore the superimposition of plots for samples of differing cross-link densities implies that the crystalline orientation is a function of the amorphous orientation prior to crystallization rather than being a function of the extension ratio or cross-link density taken separately.

In Figure 3a–c the crystalline orientation functions for the molten samples are plotted against the amorphous orientation functions as calculated by X-ray diffraction. Clearly, the plot of the lower cross-linked 3MR samples can be superimposed over the plot of the higher cross-linked 6MR samples. The implication of these results is that the crystalline orientation is indeed dependent upon the amorphous orientation of the melt prior to crystallization as given by eq 11. This result may be surprising in light of the work done by Chu et al.,[19] which concludes that the gel fraction orients independently of the sol. Clearly, the sol does become oriented when deformed in the melt, and this orientation leads to an orientation of the crystalline phase. The mechanism for this is undoubtedly physical cross-links in the form of entanglements that persist during stretching. Furthermore, similar work of Forgacs on polyethylene[31] also showed a greater correlation of the data with the whole molten system rather than just the gel fraction.

Plots of the crystalline orientation functions of the pure cross-linked gel (as calculated by the Charlesby corrected equation) versus the amorphous orientation functions are shown in Figure 4a–c. When the results for the 6MR and 3MR samples are compared, they too appeared to be su-

perimposable, although the amount of amorphous orientation in the gel is of course less than the amount in the sol plus gel.

Acknowledgment. We appreciate the support of the National Science Foundation, Division of Materials Research, and the Materials Research Laboratory of the University of Massachusetts. We are indebted to the Raychem Corp. for providing PVF_2 samples and for their irradiation.

References and Notes

(1) Lovinger, A. J. *Developments in Crystalline Polymers—1*; Bassett, D. C., Ed.; Applied Science: London, 1982; Chapter 5.
(2) Marand, H.; Stein, R. S.; Stack, G. M. *J. Polym. Sci., Part B* **1988**, *26*, 1361.
(3) Kitamaru, R.; Hyon, S. *Macromol. Polym.* **1979**, *14*, 203.
(4) Kitamaru, R.; Hyon, S. *J. Polym. Sci., Polym. Phys. Ed.* **1975**, *13*, 1085.
(5) Kawai, T.; Iguchi, M.; Tonami, H. *Kolloid Z. Z. Polym.* **1967**, *221*, 28.
(6) Choi, K.; Spruiell, J. E.; White, J. L. *J. Polym. Sci., Polym. Phys. Ed.* **1982**, *20*, 27.
(7) Kuhn, W.; Grun, F. *Kolloid Z.* **1943**, *101*, 248.
(8) Flory, P. J.; Rehner, J. *J. Chem. Phys.* **1943**, *11*, 521.
(9) Hasegawa, R.; Takahashi, Y.; Chatani, Y.; Tadokoro, H. *Polym. J.* **1972**, *3*, 600.
(10) Lando, J. B.; Olf, H. G.; Peterlin, A. J. *J. Polym. Sci. Part A-1*, **1966**, *4*, 941.
(11) Alexander, L. E. *X-Ray Diffraction Methods in Polymer Science*; R. E. Kreiger Publishing Co.: Malabar, FL, 1969.
(12) Samuels, R. J. *Structured Polymer Properties*; John Wiley and Sons: New York, 1974.
(13) Wilchinsky, Z. W. *J. Appl. Phys.* **1959**, *30*, 792.
(14) Stein, R. S.; Norris, F. H. *J. Poly. Sci.* **1956**, *21*, 381.
(15) Hashiyama, M.; Gaylord, R.; Stein, R. S. *Makromol. Chem., Suppl.* **1975**, *1*, 579.
(16) Treloar, L. R. G. *The Physics of Rubber Elasticity*, 2nd ed.; Oxford University Press: Oxford, 1958.
(17) Saunders, D. W. *Trans. Faraday Soc.* **1956**, *52*, 1414, 1425.
(18) Flory, P. J. *Statistical Mechanics of Chain Molecules*; Wiley-Interscience: New York, 1969.
(19) Chu, H. D.; Kitamaru, R.; Tsuji, W. *Polym. Lett.* **1967**, *5*, 257.
(20) Charlesby, A. *Proc. Roy. Soc. London* **1954**, *A222*, 542.
(21) Takahashi, Y.; Matsubara, Y.; Tadokoro, H. *Macromolecules* **1983**, *16*, 1588.
(22) Hyon, S.; Kitamaru, R. *Bull. Inst. Chem. Res., Kyoto Univ.* **1979**, *57*, 2.
(23) Desper, C. R. A Study of Crystallization and Orientation Mechanisms in Polyethylene. Ph.D. Thesis, University of Massachusetts, 1966.
(24) Judge, J. T.; Stein, R. S. *J. Appl. Phys.* **1961**, *32*, 2357.
(25) Keller, A.; Machin, M. J. *J. Macromol. Sci.* **1967**, *B1*, 41.
(26) Keller, A.; Machin, M. J. *Polymer Systems: Deformation and Flow*; Macmillan: London, 1968; p 97.
(27) Peterlin, A. *Structure and Properties of Oriented Polymers*; Wiley: New York, 1975.
(28) Lovinger, A. J. *J. Polym. Sci., Polym. Phys. Ed.* **1980**, *18*, 793.
(29) Stein, R. S. *J. Polym. Sci., Part A-2* **1969**, *7*, 1021.
(30) Vuks, M. F. *Opt. Spektrosk.* **1957**, *2*, 494.
(31) Forgacs, P.; Stein, R. S., unpublished, University of Massachusetts, Amherst.